PROCEEDINGS, Thirty-Eighth Workshop on Geothermal Reservoir Engineering
Stanford University, Stanford, California, February 24-26, 2014
SGP-TR-202

Application of Integrated Multicomponent Geothermometry at the Chachimbiro Thermal Area, a Difficult Geothermal Prospection Case

Fabrizio Gherardi [1] and Nicolas Spycher [2]

[1] Istituto di Geoscienze e Georisorse, Consiglio Nazionale delle Ricerche, via G.Moruzzi 1, Pisa, 56124, Italy

[2] Lawrence Berkeley National Laboratory, 1 Cyclotron Road, Berkeley, CA, 94720, USA

E-mail: f.gherardi@igg.cnr.it, nspycher@lbl.gov

Keywords: geothermometry, optimization, geothermal exploration, Chachimbiro, Ecuador.

ABSTRACT

Multicomponent geothermometry coupled with numerical optimization is applied to thermal springs of Chachimbiro, Ecuador, to gain insights on the geothermal potential of the area, and to possibly reconstruct the composition of the deep geothermal fluid. Major sources of uncertainty in the chemical prospection of the area arise from the absence of zones of upflow and boiling, which suggests that the Na–Cl thermal end-member is likely affected by mixing with Ca–HCO_3 shallow groundwater and, possibly, by degassing before discharging at the surface. Data from a previous study were used to group and select waters for application of the method. Due to the lack of detailed information on local reservoir mineralogy, different mineral assemblages and equilibration constraints have been applied to estimate thermo-chemical conditions at depth. Numerical optimization with single and multiple waters indicate deep equilibrium temperatures around 260°C, somewhat more than previous estimates (230±5°C) by classical methods. The reconstructed deep water compositions are sensitive to the optimization procedure and choice of mineral assemblage, however the range of estimated temperatures is comparatively less sensitive to these modeling constraints. The variability of results reflects the intrinsic sensitivity of the method to the mineral assemblage selected as representative of the deep reservoir, which is typically poorly known in newly prospected geothermal areas.

1. INTRODUCTION

Located in the Western Andean Range (Cordillera Occidental), about 70 km NNE of Quito, Ecuador (Fig.1A), the Chachimbiro thermal area has been investigated for geothermal prospecting since the early 80's (INECEL, 1983). Available tectonic and geovolcanological information (Aguilera, 1998) indicate that surface hydrothermal manifestations are controlled by a system of NE-SW and WNW-ESE trending faults, but the lack of comprehensive hydrogeological and geophysical studies over the thermal area *de facto* impedes identifying the depth and thickness of the reservoir, and establishing a reliable groundwater circulation model.

Based on previous geochemical investigations, the Chachimbiro thermal area has been identified as the area of highest geothermal interest in Ecuador (Almeida et al., 1992; Aguilera et al., 2005). In these previous studies, a number of warm springs and bubbling pools have been investigated by chemical geothermometry to evaluate subsurface temperature conditions, and to delineate a preliminary geochemical conceptual model of the hydrothermal system. The thermal springs located in the Chachimbiro geothermal area originate through dilution of a parent geothermal water, and seem to experience different degrees of water-rock re-equilibration at lower temperatures before discharging at the surface. The occurrence of bubbling springs with sulfur-bearing gas contents below the analytical detection limit, and sparse travertine deposits around the thermal features, suggest that gas exsolution/condensation, in addition to mineral precipitation/dissolution, might have affected the chemical signature of deep reservoir temperatures.

The waters discharged from the Na-Cl thermal springs are thought to represent the lateral outflow of a geothermal reservoir possibly located at a depth of 1000 to 2000 m East of the Cerro Albuji and Cerro Hugo volcanic complexes. Based on the application of classical mixing models, speciation calculations, and carbon-gases geochemistry, a liquid-dominated reservoir containing relatively dilute (up to 190 meq/kgw total ionic salinity) Na-Cl waters has been hypothesized at temperature values between 225 and 260°C and P_{CO2} up to about 5 bar, respectively (Aguilera et al., 2005).

The temperature and chemical composition of the geothermal parent water so far recalculated suffers from the inherent limitations of classical methods to explicitly account for the geochemical impact of secondary processes, such as dilution, mixing, and degassing, on the chemical signature of fluids ascending from deep geothermal reservoirs. In order to gain further insights on this geothermal reservoir, and to eventually pinpoint an equilibrium mineralogical assemblage controlling the chemical composition of fluids at depth, the recently developed multicomponent geothermometry approach developed by Spycher et al. (2011, 2014) has been applied to a selected number of thermal springs.

2. GEOLOGICAL SETTING

The Andean Range, South America, is the result of the subduction of the Nazca Plate beneath the South American Plate. In Ecuador, the Andean Range is constituted by two parallel mountain chains, the Cordillera Occidental to the west, and the Cordillera Real to the east, separated by an almost flat depression called the Interandean Depression (Aguilera, 1998; Fig.1A). The western Cordillera is mainly formed by basic and intermediate volcanic rocks, covered by discontinuous layers of turbiditic deposits, whereas the Cordillera Real is made of intrusive and sedimentary rocks, metamorphosed at a later stage. The Interandean Depression is a tensional structure of regional importance bounded by active normal faults and filled by volcanic and volcano-sedimentary deposits several thousand meters thick. The uneven topography of the Chachimbiro area is characterized by the

presence of the Huanguillaro volcanic complex, a major volcanic structure that includes the Cotacachi, Pilavo, Yanaurco de Piñán and Cerro Negro volcanic vents, and several acid domes emplaced less than 8,000 years ago (Fig.1B). Highly differentiated volcanic products spanning from andesites to rhyodacites, together with significant volumes of pyroclastic deposits, dominate the local geology (Aguilera,1998).

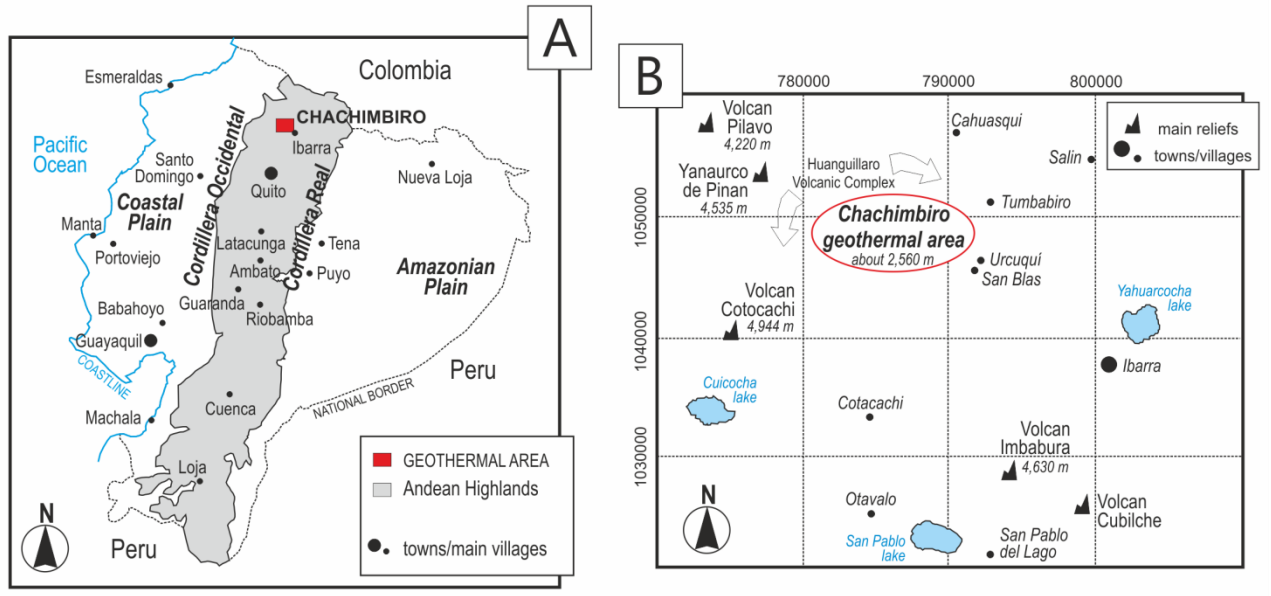

Figure 1 – Location map of the Chachimbiro geothermal area (A), with indication of the main volcanic reliefs and the average altitude of the geothermal prospect area (B).

3. CHEMICAL AND ISOTOPIC COMPOSITION OF THERMAL WATERS

The chemical and isotopic composition of hydrothermal fluids from Chachimbiro has been described by Almeida et al. (1992) and Aguilera et al. (2005). Thermal springs have a Na-Cl to Na-Cl-HCO_3 signature, different from low-salinity, Ca-HCO_3 waters from creeks and cold springs (Fig.2A). The occurrence of mixing between these two end-members (line marked "dilution trend" of Fig. 2A) is supported by a number of strong correlations between distinct chemical constituents and chloride, used in this framework as a conservative reference component. However, many thermal spring waters fall off this mixing trend (Figs. 2A, 2B), presumably as the result of secondary processes. The chemical composition of a number of these waters, characterized by comparatively high concentrations of Mg, Ca, and HCO_3, has been interpreted as the result of CO_2-driven rock-dissolution processes along the ascending path from the reservoir. Waters characterized by relatively low Ca contents have likely experienced secondary precipitation of calcium-bearing minerals, presumably calcite, during their underground circulation path.

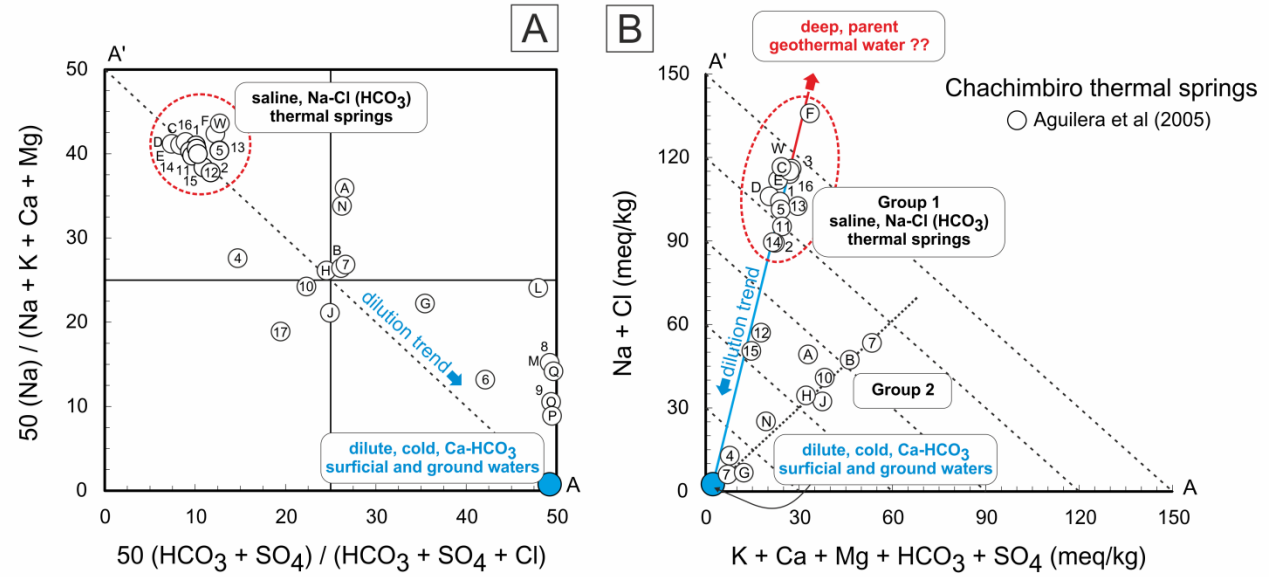

Figure 2 – Langelier-Ludwig diagram (A) and related salinity diagram (B), for Chachimbiro thermal springs. A number of thermal springs (red envelope; box A) are thought to be representative of the main outflow of the geothermal reservoir. Two main groups of thermal waters have been identified (B), and separately subjected to multicomponent geothermometry computations. Spring are labeled as in Table 1 of Aguilera et al. (2005).

Surficial waters and low-Cl, cold springs have a typically meteoric $\delta^{18}O$-$\delta^{2}H$ signature, and plot close to the worldwide meteoric water line. In contrast, the stable isotope composition of thermal springs reflects the significant contribution of a deep-seated component, possibly related to both the inflow of arc-type magmatic waters (Giggenbach, 1992) and the enhanced water/rock exchange of oxygen isotopes under reservoir conditions (the so-called "oxygen-shift"). Aguilera et al. (2005) showed a strong linear correlation between the Cl content and $\delta^{18}O$ values of the most-isotopically shifted thermal waters, which is additional evidence in support of a groundwater circulation model controlled by the mixing between local meteoric waters and hydrothermal fluids deriving from a single geothermal reservoir.

4. NUMERICAL APPROACH

In this study we continue the development and application of the integrated multicomponent geothermometry approach recently presented by Spycher et al. (2011, 2014). This approach relies on the mineral saturation index method originally developed by Reed and Spycher (1984), coupled with numerical optimization. Over a given temperature range of interest (e.g., 100–300°C), the reservoir temperature is inferred from the clustering of mineral saturation indices near zero, for a group of minerals representative of the reservoir mineralogical assemblage. These geothermometry computations are implemented into a stand-alone computer program (GeoT) that automatically assesses the clustering of mineral saturation indices, and determines the temperature at which the clustering near zero is optimal. This allows the coupling of GeoT with itough2 using the PEST protocol (Finsterle et al, 2011) to estimate unknown or poorly known input parameters necessary to reconstruct the deep water composition, such as the amount of mixing with shallow dilute waters and/or amount of degassing. In doing so, this approach allows the estimation of reservoir temperatures based on the reconstructed deep fluid composition. Spring waters that are suspected to originate from a common deep reservoir can be processed simultaneously to constrain the optimization.

Here we follow an approach similar to Peiffer et al. (2014), who applied this method to well and spring waters from Dixie Valley, Nevada, by grouping waters according to their chemical and isotopic composition, then processing each group separately. In the present case, a set of chemical and isotopic data is available (Aguilera et al., 2005) to group water composition using classical methods. Principal component analyses have also been conducted as part of the present study for this purpose. Two main groups were identified (Fig. 2B): Group 1, which consists of the majority of the thermal springs and falls on the main dilution trend, and Group 2 representing a smaller group of waters following a different trend, likely from dilution and secondary reactive processes. One spring sample (#1) suspected to be among the closest in composition to the deep reservoir fluid was first processed (individually) to test mineralogical constraints most likely relevant to the deep reservoir. Selected waters from each group were then processed simultaneously using this information, with details given below.

The geothermometry method relies heavily on the selected mineral assemblage, and on water analyses that are as complete and accurate as possible, including Al concentration (e.g., Pang and Reed, 1998). In the present case, little is known on the deep reservoir and its alteration mineralogy, and reported analyses do not include trace metals such as Al and Fe, or species that can be used to assess the redox state of the system (SO_4 is reported but not HS, which oxidized). For this reason, we initially used spring sample #1 to test several mineral assemblages, and various thermodynamic constraints to fix the concentrations of some aqueous species. Best results were obtained by selecting a mineral assemblage consisting of albite (albit-lo), k-feldspar (microcli), chlorite (clchlore), muscovite, quartz, heulandite, pyrite, magnetite and anhydrite. Al was constrained by K-feldspar, Mg by chloride, Fe by magnetite, and dissolved sulfide by pyrite. Epidote and montmorillonite were also considered but not found to cluster as well as the other minerals. Using these mineralogical constraints, the unknown dilution factor and steam fraction of discharge were estimated by numerical optimization with GeoT coupled to itough2, using a grid-search minimization procedure (Finsterle, 2007). The gas composition necessary to reconstruct the deep fluid was taken as an average of (consistent) analyses reported for a few springs by Aguilera et al. (2005), normalized to remove small detected quantities of O_2 and N_2.

After applying this approach to spring water #1, waters from each of the two identified groups of spring were processed simultaneously. This was accomplished using the same mineral assemblage and constraints as mentioned above, but this time solving for a dilution factor and gas fraction for each spring. Samples from five springs were selected from each group. In this case, because of the large number of unknowns, a grid-search minimization procedure could no longer be applied. Instead, a Simplex minimization procedure was applied, in some cases followed by a localized Levenberg-Marquardt procedure (see Finsterle, 2007 for details on these procedures). These methods have more potential for converging towards false minima than mostly "fool-proof" grid-search minimization. Therefore, successful optimizations required several trials, testing different optimization input parameters (i.e, different initial trial values of unknown parameters, and weighting factors).

5. RESULTS

A temperature of about 260±6°C was estimated with sample #1, with fairly good clustering of the selected minerals at this temperature, spreading 246–266°C (Fig. 3). This contrasts with temperatures evaluated using classical geothermometers for un-reconstructed waters (T_{quartz} 148–186°C, $T_{Na\text{-}K}$ 150–236°C, and $T_{K\text{-}Mg}$ 89–119°C; Aguilera et al., 2005). The optimization procedure yields a dilution factor of ~2.3, gas weight fraction of discharge around 17 wt%, and a reconstructed deep water with a pH ~6.4 and P_{CO2} ~18 bar. The pH is in line with previous estimates by Aguilera et al. (2005), but the P_{CO2} is more than three times higher than the value estimated by these authors (5 bar). It was found, however, that waters of quite variable reconstructed carbonate concentrations, pH and P_{CO2} all yielded similar temperatures in the range ~ 240–270°C, because for this system the temperature estimates are much less sensitive to the gas fraction (consisting primarily of H_2O+CO_2) than to the dilution factor.

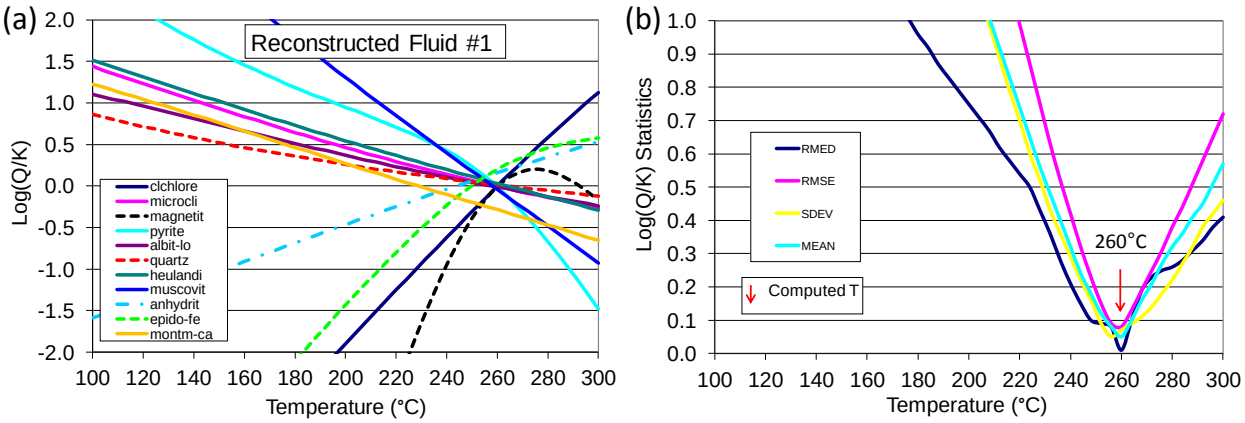

Figure 3 – Multicomponent geothermometry using thermal spring #1 (Aguilera et al., 2005). (a) Computed saturation indices (SI) graphed as a function of temperature; the clustering near zero occurs around 260°C. (b) Measure of clustering: median (RMED), mean root square error (RMSE), standard deviation (SDEV) and average (MEAN) of absolute SI values. The equilibrium temperature is inferred from the temperature at which RMED is minimum (Spycher et al., 2014).

By processing multiple waters simultaneously, the variability of reconstructed water compositions was narrowed down, however the optimization became more challenging because of the increased number of parameters requiring estimation (i.e., different dilution factors and gas fractions for each spring). Five analyses of waters from Group 1 (#1, 2, 3, 5, and C) were processed simultaneously, yielding an average temperature of 261°C, with individual water temperatures ranging from 254±18°C (for #3) to 268±11°C (for #2) (Table 1). Five waters from Group 2 (#7, 10, B, H and N) were also processed simultaneously. In this case, the optimization was more difficult than for Group 1, requiring a fair number of trials until a reasonably narrow range of temperatures was estimated for all springs. An average temperature of 251°C was obtained, with individual water temperatures ranging from 244±14°C (for #H) to 258±30°C (for #7) (Table 1, Fig. 4). The reconstructed water compositions and temperatures for both groups are shown on Table 1. Example of saturation index plots are shown in Fig. 4. for the springs showing the highest estimated temperature in each group.

Table 1 – Estimated temperatures and deep water compositions reconstructed by numerical optimization for springs in Group 1 and Group 2 (spring names and labels correspond to those in Table 1 of Aguilera et al., 2005).

GROUP 1	Spring =	101	102	103	105	EUI_02
	Label =	1	2	3	5	C
Estimated Temperature (°C) =		266	268	254	256	260
Concentration Factor =		2.0	2.04	1.98	1.77	2.15
Gas (weight %) =		0.10%	9.70%	0.80%	0.30%	0.40%
pH (at T) =		7.50	6.70	7.10	7.50	7.50
P_{CO2} (bar) =		1.30	9.40	2.60	0.87	1.20
Cl (mg/kgw) =		3708	2967	4075	3208	4387
SO_4 (mg/kgw) =		69	58	58	64	65
C(+4) as HCO_3 (mg/kgw) =		1558	7908	2731	1174	1722
S(-6) as HS (mg/kgw) =		86	24	37	70	96
SiO_2 (mg/kgw) =		435	393	362	383	391
Al (mg/kgw) =		0.19	0.27	0.23	0.18	0.23
Ca (mg/kgw) =		162	162	202	154	204
Mg (mg/kgw) =		0.00038	0.0036	0.0011	0.00035	0.00036
Fe (mg/kgw) =		0.0055	0.0021	0.0030	0.0050	0.0061
K (mg/kgw) =		282	232	232	257	290
Na (mg/kgw) =		2373	1886	2629	2048	2904
B (mg/kgw) =		89	71	10	76	107
Classical Geothermometry		Temperature (°C) using reconstructed deep fluid				
Quartz (Fournier & Potter 1982)		243	233	226	231	233
Na-K-Ca (Fournier & Truesdell 1973)		222	219	203	223	213
Na-K (Giggenbach 1988)		246	249	222	251	229
K-Mg (Giggenbach 1988)		503	373	427	497	511

GROUP 2	Spring =	110	EUI_01	113	EUI_6	EUI_31
	Label =	7	B	10	H	N
Estimated Temperature (°C) =		258	252	250	244	248
Concentration Factor =		2.11	2.42	2.98	2.89	4.2
Gas (weight %) =		0.10%	0.10%	5.31%	2.30%	1.80%
pH (at T) =		7.46	7.61	6.57	6.76	6.97
P_{CO2} (bar) =		2.83	2.76	13.06	3.53	6.47
Cl (mg/kgw) =		1870	1642	2220	1754	1666
SO_4 (mg/kgw) =		23	24	124	32	9
C(+4) as HCO_3 (mg/kgw) =		3904	4816	10547	2959	5928
S(-6) as HS (mg/kgw) =		79	96	11	13	22
SiO_2 (mg/kgw) =		392	406	407	365	470
Al (mg/kgw) =		0.29	0.20	0.13	0.20	0.22
Ca (mg/kgw) =		502	600	625	197	254
Mg (mg/kgw) =		0.00038	0.00036	0.0085	0.0023	0.0016
Fe (mg/kgw) =		0.0050	0.0062	0.0019	0.0018	0.0022
K (mg/kgw) =		134	153	164	98	55
Na (mg/kgw) =		1397	1608	1245	1099	1345
B (mg/kgw) =		56	60	48	42	
Classical Geothermometry		Temperature (°C) using reconstructed deep fluid				
Quartz (Fournier & Potter 1982)		233	236	239	227	251
Na-K-Ca (Fournier & Truesdell 1973)		187	188	205	188	149
Na-K (Giggenbach 1988)		229	228	222	224	170
K-Mg (Giggenbach 1988)		424	439	409	325	299

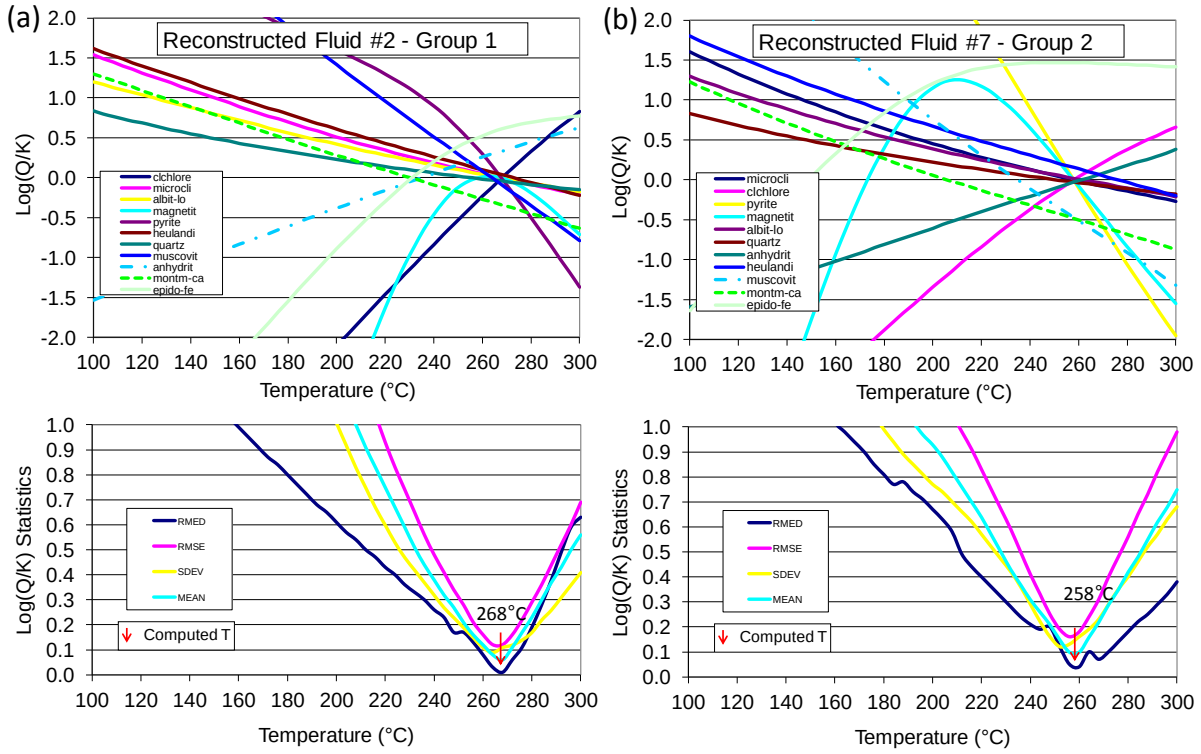

Figure 4 – Multicomponent geothermometry using multiple thermal springs (Table 1) selected from the two groups shown on Fig. 2B. Example results for springs with highest estimated temperatures in (a) Group 1 and (b) Group 2.

These preliminary results suggest similar deep temperatures for both groups, with Group 2 displaying somewhat lower values and more scatter than Group 1. The larger scatter is to be expected given that samples from Group 2 appear to have undergone more dilution than those from Group 1. The reconstructed waters from Group 2 show noticeably lower salinities than Group 1, which could be the caused by re-equilibration of the deep fluid after some dilution occurred. A noticeable difference with previous interpretations (Aguilera et al., 2005) is the higher pH and Ca concentration, and lower P_{CO2} estimated for many of the springs (which causes significant calcite supersaturation). As noted earlier, the computation results are not as sensitive to the gas fraction as they are to the dilution factor, and therefore over- or under-estimations of P_{CO2} (and pH) cannot be ruled out. The absence of carbonate minerals in the selected mineral assemblage also likely contributes to this low sensitivity. However, tests including carbonate minerals did not yield as consistent temperatures. Another observation from Table 1 is the quite small Mg concentrations, which indicate that a phase less stable than clinochlore may be more suitable to fix the Mg concentrations at depth in this system. As a result, the K-Mg temperatures estimated with the reconstructed waters are unrealistically high (Table 1). In the present case, a reasonably narrow range of reservoir temperatures is obtained for the five springs (244–268°C), and somewhat higher than the range of Na-K and Na-K-Ca temperatures obtained with the reconstructed fluid compositions (Table 1).

6. SUMMARY AND CONCLUSIONS

At Chachimbiro, Ecuador, the discharge of pH-neutral, Na-Cl and Na-Cl-HCO_3 thermal springs is interpreted as the lateral outflow of a high-temperature, liquid dominated geothermal system. Previous geochemical prospecting (Almeida et al., 1992; Aguilera et al., 2005) indicated that secondary processes, such as mixing with cold, surficial waters, secondary mineral precipitation and degassing, control of the chemical signature of hydrothermal waters during their ascent from the geothermal reservoir. The reconstruction of the deep parent water at Chachimbiro is further complicated by the absence of major upflow and degassing zones, i.e., by the lack of surface manifestations directly representative of thermo-chemical conditions at depth, and by the lack of information on the deep alteration mineral assemblage.

Based on a subset of selected chemical analyses, multicomponent geothermometry coupled with numerical optimization has been applied at Chachimbiro to estimate the extent of dilution and degassing processes, to evaluate potential mineralogical assemblage controlling the fluid chemistry at depth, and possibly define the equilibrium temperature of the reservoir. The results of this approach are sensitive to the minerals considered in the calculations. Best results were obtained by selecting a mineral assemblage consisting of albite, microcline, clinochlore, muscovite, quartz, heulandite, pyrite, magnetite and anhydrite, which are common minerals in high-temperature (and propylitically) altered rocks. The reconstructed parent-water equilibrium temperatures for the two groups of springs were found to range ~250–270°C for Group 1 and ~240–260°C for Group 2. These temperatures are somewhat higher than previously estimated (up to ~235°C) by classical geothermometry, but in line with estimates >260°C suggested by Aguilera et al. (2005) using CO_2-CH_4-CO equilibria. The deep compositions of the spring waters were estimated by numerical optimization, yielding salinities for Group 1 roughly double those estimated for Group 2, suggesting potential re-equilibration of Group 2 waters after dilution.

The study of Aguilera et al. (2005) aimed at reconstructing the deep parent-water composition at Chachimbiro using more standard methods than done here, and thus provides a basis to assess the approach followed in the present study. However, it is difficult to verify either method in absence of actual subsurface data. The reconstructed compositions for Group 1 springs are more saline (~4400 ppm Cl maximum) than the deep fluid composition estimated by Aguilera et al. (2005) (2250 ppm Cl) but generally follow the trend of these data, with the noticeable exception of higher pH, Ca, and total dissolved carbonate content, and much lower Mg concentrations. These differences possibly reflect insufficient and/or inappropriate constraints applied during the minimization procedure, or a prevailing alteration mineralogy in the deep reservoir that is different than assumed here. Therefore, the deep fluid compositions estimated in this study should be considered preliminary, as we continue the refinement of the numerical approach and the testing of additional minimization procedures most suitable for simultaneous optimization of multiple waters with multiple minerals. Nevertheless, despite these uncertainties, this study highlights the potential of this new approach for processing water chemical analyses in a more integral manner than using classical geothermometers alone, most particularly when thermal spring waters have been subjected to significant mixing and degassing before discharging at the surface.

REFERENCES

Aguilera, E.: The Chalupas and Chachimbiro Geothermal Fields in Ecuador, *Geothermal Resources Council Transactions*, **22**, (1998), 247-251.

Aguilera, E., Cioni, R., Gherardi, F., Magro, G., Marini, L., and Pang, Z.: Chemical and isotope characteristics of the Chachimbiro geothermal fluids (Ecuador), *Geothermics*, **34**, (2005), 495–517.

Almeida, E., Sandoval, G., Panichi, C., Noto, P., and Bellucci, L.: Modelo geotérmico preliminar de areas volcanicas del Ecuador a partir de estudios químicos e isotópicos de manifestaciones termales (*in spanish*). In: IAEA-TECDOC-641, Geothermal investigations with isotope and geochemical techniques in Latin America, Proceedings of the Final Research Co-ordination Meeting held in San José, 12–16 November 1990, Costa Rica, (1992), 219-236.

Finsterle, S., iTOUGH2 User's Guide, Lawrence Berkeley National Laboratory, Report LBNL-40040, February 2007, 130 pp.

Finsterle, S., and Zhang, Y.: Solving iTOUGH2 simulation and optimization problems using the PEST protocol. *Environmental Modeling and Softw*are, **26**, (2011), 959–968,http://dx.doi.org/10.1016/j.envsoft.2011.02.008.

Fournier, R.O., and Potter, R.W.: A revised and expanded silica (quartz) geothermometer. *Geothermal Resources Council Bulletin*, **11** (10), (1982), 3–12.

Fournier, R.O., and Truesdell, A.H.: An empirical Na–K–Ca geothermometer for natural waters. *Geochimica et Cosmochimica Acta*, **37**, (1973), 1255–1275.

Giggenbach, W.F.: Isotopic shifts in waters from geothermal and volcanic systems along convergent plate boundaries and their origin. *Earth and Planetary Science Letters* **113**, (1992), 495–510.

Giggenbach, W.F., 1988. Geothermal solute equilibria. Derivation of Na–K–Mg–Ca geoindicators. *Geochimica et Cosmochimica Acta*, **52**, 2749–2765.

INECEL: Sintesis de los Estudios de Aprovechamiento de los Recursos Geotérmicos en el Area de Chalupas. Unpublished internal report (*in spanish*), (1983).

Pang, Z.-H., Reed, M.H.: Theoretical chemical thermometry on geothermal waters: problems and methods. *Geochimica et Cosmochimica Acta*, **62**, (1998), 1083–1091.

Peiffer, L., Wanner, C., Spycher, N., Sonnenthal, E., Kennedy, B.M., and Iovenitti, J.: Optimized multicomponent vs. classical geothermometry: insights from modeling studies at the Dixie Valley geothermal area. *Geothermics* **51**, (2014), 154–169.

Reed, M.H., Spycher, N.F., 1984. Calculation of pH and mineral equilibria in hydrothermal waters with application to geothermometry and studies of boiling and dilution. *Geochimica et Cosmochimica Acta*, **48**, 1479–1492.

Spycher, N., Sonnenthal, E., Kennedy, B.M.: Integrating multicomponent chemical geothermometry with parameter estimation computations for geothermal exploration. *Geothermal Resources Council Transactions*, **35**, (2011), 663–666.

Spycher, N.F., Peiffer, L., Sonnenthal, E.L., Saldi, G., Reed, M.H., Kennedy, B.M.: Integrated multicomponent solute geothermometry), *Geothermics*, **51**, (2014), 113–123.